Disorder effects in the $S=1$ antiferromagnetic spin ladder CaV_2O_4

S.R. Guitarra [a], A. Caneiro [b], D. Niebieskikwiat [a],*

[a] Colegio de Ciencias e Ingeniería, Universidad San Francisco de Quito, Quito, Ecuador
[b] Instituto Balseiro - Centro Atómico Bariloche, 8400 Bariloche, Argentina

ARTICLE INFO

ABSTRACT

We study the physical properties of the antiferromagnetic spin ladder CaV_2O_4 (CVO) and the Y-doped related compound $Ca_{0.9}Y_{0.1}V_2O_4$. In the latter, X-ray diffraction demonstrates the segregation of a small amount of a vanadium–perovskite impurity phase, leading to the formation of V vacancies within the main CVO-type structure. The 1D character of this calcium–vanadite enhances the influence of the vacancies on the electric and magnetic properties of $Ca_{0.9}Y_{0.1}V_2O_4$. Electrical transport is characterized by a variable-range hopping mechanism determined by the charging energy of nm-sized segments of V chains delimited by V vacancies, i.e. a Coulomb gap is formed at the Fermi level. These vacancies also locally affect the magnetic correlations, breaking the long-range AFM order observed in CaV_2O_4 and producing exchange bias when the Y-doped sample is cooled with an applied magnetic field.

1. Introduction

Low dimensional and frustrated spin systems have long attracted the interest of condensed matter physicists due to the fundamental physics involved. The intricate ground states of these systems have challenged theorists to find new calculation methods to solve basic spin Hamiltonians [1]. A well known example is the CaV_2O_4 compound, with the orthorhombic AB_2O_4 calcium ferrite-type structure [2–7] (A is typically a divalent alkaline earth and B a trivalent transition metal). V^{3+} ions ($3d^2$ electronic configuration) are located inside edge sharing O_6 octahedra, forming $S=1$ zig-zag chains with competing nearest-neighbor and second-nearest-neighbor antiferromagnetic (AFM) interactions, J_ℓ and J_z, respectively (see Fig. 1). While J_ℓ arises from the direct exchange between electrons in the low energy d_{xy} orbitals along the legs of the chains, J_z results from the exchange between electrons in the high energy d_{xz} (or d_{yz}) orbitals in different legs. In this context, a gapless magnetic configuration dominated by frustrated interactions has been proposed for CaV_2O_4 [3,8]. However, other results support a gapped AFM ground state [4–9]. Moreover, recent neutron diffraction experiments suggest that a low temperature monoclinic distortion (below ∼110–140 K) modifies the orbital occupancy of the V t_{2g} levels, driving the system into a non-frustrated $S=1$ AFM spin ladder ground state [5,6]. In this case, where long-range order is proposed, disorder effects are expected to be important.

Electrical transport experiments show that CaV_2O_4 is strongly insulating even in the high temperature orthorhombic phase [10], where the degenerate d_{xz} and d_{yz} orbitals share only one single electron (see Fig. 1). In NaV_2O_4, the $3d^{1.5}$ electronic configuration of $V^{3.5+}$ is equivalent to the removal of half of these electrons, resulting in metallic conductivity along the V zig-zag chains [10–12]. The origin of such differences in the electrical properties between the Ca and Na counterparts of this vanadite, whether related to structural variations or electron–electron interactions, is still unclear. Therefore, CaV_2O_4 shows the typical challenges of strongly correlated materials, i.e. a complex interplay between spin, charge, lattice, and orbital degrees of freedom.

One effective way to study the electronic phases of low dimensional strongly correlated systems is by introducing disorder. In this paper we manipulate the ground state of CaV_2O_4 (CVO) by means of replacing Ca with Y, i.e. we study the (nominal) compound $Ca_{0.9}Y_{0.1}V_2O_4$ (CYVO). Through the segregation of an impurity phase, this replacement introduces V vacancies, i.e. disorder, within the 1D CVO-type structure. The resulting electrical conductivity exhibits clear signatures of electronic transport in a 1D disordered media, with charge excitations dominated by long range Coulomb interactions. Furthermore, the modified magnetic interactions around the V vacancies in CYVO promote local ferromagnetic (FM) correlations that break the long-range order of the AFM spin ladders observed in the undoped material.

* Corresponding author.
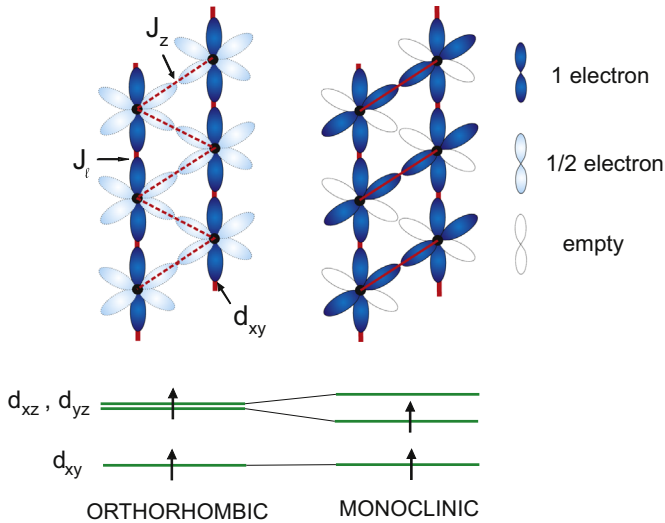E-mail address: dniebieskikwiat@usfq.edu.ec (D. Niebieskikwiat).

Fig. 1. Occupancy of V t_{2g} orbitals in CaV$_2$O$_4$ according to Pieper et al. [6]. A low temperature monoclinic distortion unbalances the electron population of the d_{xz} and d_{yz} orbitals, leading to the AFM spin-ladder ground state.

2. Sample preparation and characterization

Polycrystalline CVO and CYVO samples were synthesized from stoichiometric mixtures of CaCO$_3$, metallic V, and Y$_2$O$_3$. The raw materials were dissolved in nitric acid. After evaporation, citric acid and ethylene glycol were added and the solution was dried again to obtain the precursor powders. After grinding, the powders were calcined at 500 °C in air for 72 h followed by a second treatment at 900 °C for 12 h in a H$_2$(10%)/Ar environment. Then the powders were pressed into pellets and sintered at 1200 °C for 24 h in a H$_2$(10%)/Ar atmosphere. Powder X-ray diffractograms for both samples were recorded on a Phillips PW 1700 diffractometer using Cu Kα radiation and a graphite monochromator.

For the CVO sample, X-ray diffraction analysis shows a single phase orthorhombic material (*Pbnm* space group) with lattice parameters $a = 10.6877(2)$ Å, $b = 9.2182(2)$ Å, and $c = 3.0136(1)$ Å. In the Y-doped sample, Rietveld refinements show that this orthorhombic structure keeps very similar lattice parameters [$a = 10.6909(2)$ Å, $b = 9.2143(2)$ Å, and $c = 3.0080(1)$ Å]. However, CYVO is not single phase, and the calcium ferrite-type structure coexists with a minor but noticeable amount of impurities of the orthorhombically distorted perovskite Y$_{0.7}$Ca$_{0.3}$VO$_3$ [13]. As shown by the X-ray diffractogram in Fig. 2, two small peaks can be observed at $2\theta \sim 48°$ associated with the (220) and (004) Bragg reflections of Y$_{0.7}$Ca$_{0.3}$VO$_3$, which also belongs to the *Pbnm* space group. From the high quality Rietveld refinement shown along with the diffraction data, we obtained the lattice parameters of this impurity phase as $a = 5.305(2)$ Å, $b = 5.543(2)$ Å, and $c = 7.585(2)$ Å (similar to its bulk lattice parameters, Ref. [13]), and an impurity content of 2.42 (9)% weight fraction could also be determined. The fact that Bragg peaks are observed indicates that this is a physically segregated phase, however, due to the small amount and AFM character of Y$_{0.7}$Ca$_{0.3}$VO$_3$, this impurity does not affect the transport and magnetization measurements. Actually, no hints are observed in our data at the relevant transition temperatures of this perovskite [13,14]. However, we shall demonstrate that the segregation of this impurity has important implications on the physical properties of the main calcium–vanadite phase in the CYVO sample.
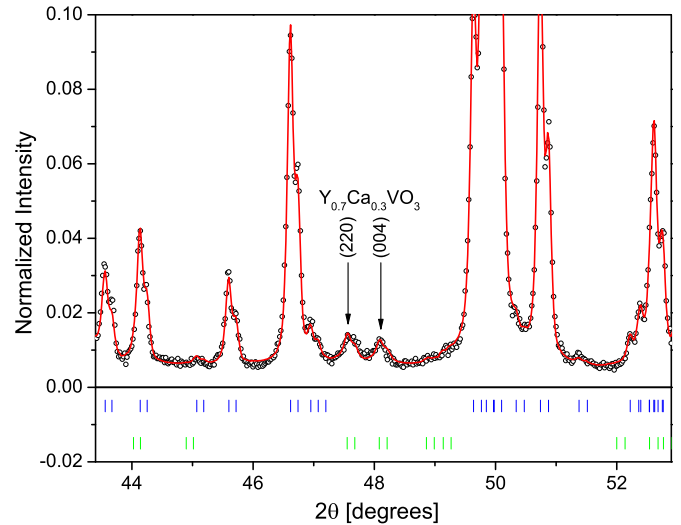

Fig. 2. X-ray diffractogram of the Ca$_{0.9}$Y$_{0.1}$V$_2$O$_4$ sample (open circles: experimental data, red line: Rietveld refinement, blue bars: Bragg reflections of the CVO-type phase, green bars: Bragg reflections of the Y$_{0.7}$Ca$_{0.3}$VO$_3$ impurity phase). The arrows indicate two reflections that correspond to this perovskite impurity phase. (For interpretation of the references to color in this figure caption, the reader is referred to the web version of this paper.)

3. Results and discussion

3.1. Electrical transport properties

Fig. 3 shows the high temperature (orthorhombic phase) electrical resistivity of the CVO and CYVO samples, measured in the standard four-probe configuration. Although in both cases we obtained an insulating response, neither of the samples follow the usual activated behavior, $\rho(T) \propto Te^{T_0/T}$. Instead, our resistivity curves are well described by $\rho(T) \propto Te^{(T_0/T)^\beta}$. This behavior has been usually ascribed to variable-range hopping (VRH) transport, where electrons hop between energetically convenient localized states in a disordered system. Originally developed for isotropic doped semiconductors, the characteristic exponent for 3D disordered systems takes the value $\beta = 1/4$, i.e. the so-called Mott law [15]. Efros and Shklovskii (ES) then extended Mott's arguments to
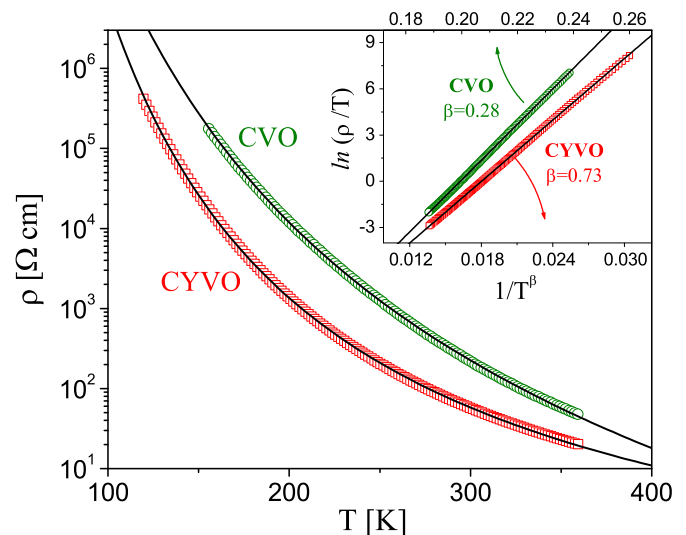
Fig. 3. Electrical resistivity as a function of temperature for Ca$_{0.9}$Y$_{0.1}$V$_2$O$_4$ and CaV$_2$O$_4$. The VRH law $\rho(T) \propto Te^{(T_0/T)^\beta}$ (black lines) satisfactorily describes the data over several orders of magnitude of change of ρ. Inset: linear relationship of $\ln(\rho/T)$ vs. $1/T^\beta$.

include the long-range electron–electron Coulomb interactions, and found the ES law $\beta = 1/2$ [16]. None of these two exponents describe satisfactorily our CYVO sample, where the experimental exponent is $\beta \approx 0.73$ (see Fig. 3). Nonetheless, more recently Fogler et al. studied the VRH mechanism in the context of the emerging quasi-1D systems, including disorder and anisotropic long-range Coulomb interactions in a 3D arrangement of parallel 1D chains [17]. In that paper, the authors considered point defects that divide the 1D chains into small pieces of length ℓ, the average distance between defects. In this system, charge transport proceeds *via* tunneling of electrons between different segments of the 1D chains. These charge excitations, i.e. addition or removal of electrons from one of these segments, imply a Coulomb energy that produces a "soft" Coulomb gap in the density of states at the Fermi level, i.e. $g(\varepsilon) \sim |\varepsilon - \varepsilon_F|^\mu$ [18]. On this ground, the authors found that the VRH exponent takes the value [17]

$$\beta = \frac{(\mu + 1)}{(\mu + d + 1)} \tag{1}$$

where d is the effective dimensionality of the tunneling process ($d = 1$, 2 or 3, depending on the localization length perpendicular to the chains). The exponent μ, which characterizes the physical situation of each individual system and increases with the density of defects, can take the values 0, 1 or 2. Although Fogler's model was developed to study the charge transport along the 1D chains, in polycrystalline systems where crystalline orientations are randomly distributed, electrons would flow following the best electrical paths. Since CaV_2O_4 is extremely anisotropic, this means that the current would flow along intricate paths, always following the direction of the V chains. Hence, these paths would be determined by the relative orientation of neighboring grains, only introducing a geometrical factor in the resistivity of the material, similar to that of percolation theory [19]. Therefore, with the current still flowing along the V chains, we expect that Fogler's model is still very useful to analyze the temperature dependence of the resistivity of our CVO and CYVO samples.

Within this framework, an exponent $\beta = 3/4$ is naturally obtained by considering $d = 1$ and $\mu = 2$. This is thus the situation of our CYVO compound ($\beta \approx 0.73$), where tunneling of electrons perpendicular to the chains is indeed expected to be unlikely [11,12]. However, the quadratic dependence of the density of states ($\mu = 2$) indicates a large Coulomb gap around the Fermi level. This corresponds to the ES regime, which occurs at large concentrations of point defects [17]. Therefore, CYVO must be regarded as a strongly disordered 1D system.

The origin of such point defects in CYVO is in fact correlated to the segregation of the perovskite impurity phase. When this impurity is formed, A and B ions abandon the main AB_2O_4 calcium ferrite-type phase, leaving the corresponding vacancies within this structure. In a single phase (defect-free) $Ca_{0.9}Y_{0.1}V_2O_4$ compound, the replacement of 10% of Ca^{2+} with Y^{3+} would have changed the V average oxidation state from +3 to +2.95, thus CYVO would have had a concentration of 5% of V^{2+} ions. Instead of this, the CYVO sample segregates $Y_{0.7}Ca_{0.3}VO_3$ impurities, thus removing positively charged Y and V ions and avoiding the formation of V^{2+} within the CVO-type structure. Indeed, the bond valence sum rule shows no evidence of V^{2+} in our CYVO sample. This is in fact expected due to the large ionic radius of V^{2+}, which would not fit within the O_6 octahedra without producing excessive structural strain (the ionic radius of V^{2+} is 0.79 Å,~ 23% larger than that of V^{3+}).

From the weight fraction of $Y_{0.7}Ca_{0.3}VO_3$ obtained from X-ray diffraction, the molar fraction of impurities is calculated to be 2.9 (1)%, i.e. instead of $Ca_{0.9}Y_{0.1}V_2O_4$ we have

$$(97.1\%) \; Ca_{0.899}Y_{0.080}V_{1.987}O_4 + (2.9\%) \; Y_{0.7}Ca_{0.3}VO_3 \tag{2}$$

From this equation, the calculated concentration of V vacancies is ~0.65%, meaning that there is one V vacancy every ~154 V sites, i.e. there is one vacancy every ~77 rungs of the V ladders. The V–V distance along the legs in Fig. 1 is $c = 3.008$ Å, thus the average distance between V vacancies along the two-leg ladders is ~23 nm. In a 3D system, this small concentration of vacancies would likely have negligible effects on the physical properties. On the contrary, the 1D character of the V chains makes these vacancies play a key role in the physics of CaV_2O_4.

For the electrical transport in CYVO, the V vacancies are playing the role of point defects within the quasi-1D V chains, and the VRH mechanism with the exponent $\beta \approx 0.73$ is observed. Remarkably, this VRH law holds for our calcium–vanadite system in a broad range of resistivities and temperatures, more than four orders of magnitude and 200 K, respectively (see Fig. 3). Therefore, we conclude that V vacancies are indeed cutting the V chains into short pieces of length $\ell \approx 23$ nm, where electrons are added or removed in the transport process. Also, the agreement between our data and Fogler's VRH theory demonstrates that electron–electron correlations greatly affect the transport properties of calcium–vanadites, and likely prevent metallic conductivity in the t_{2g} bands of the orthorhombic CaV_2O_4. This would be similar to the results obtained in some spinel compounds, such as ZnV_2O_4 [20]. Indeed NaV_2O_4, with the same crystalline structure and orbital configuration than CaV_2O_4, but half the electron concentration in the electrically active d_{xz} and d_{yz} orbitals, shows metallic conductivity [10–12].

Finally, Fogler's VRH theory can also account for the counter-intuitive situation where the cleaner sample (CVO) exhibits a resistivity an order of magnitude larger than that of the dirty sample (CYVO), as shown in Fig. 3. We note, however, that in this case the CVO sample should be described by the Mott law, where the density of states at the Fermi level remains finite, i.e. $\mu = 0$ and $\beta = 1/2$ for a 1D tunneling process [17]. However, the experimental exponent $\beta \approx 0.28$ is well below the expected value, and much closer to the 3D Mott exponent $\beta = 1/4$. This observation implies that clean CaV_2O_4 is not completely one-dimensional, but must be considered within a highly anisotropic 3D-like Mott regime. On the contrary, CYVO exhibits a truly 1D charge transport. This change in the dimensionality of the system is probably related to the structural changes of the calcium–ferrite-type phase when Y-doping is introduced. To illustrate these changes, in Table 1 we present the different V–V distances for both samples, obtained from the Rietveld refinements. The first four lines in this table show that all the intra-chain V–V distances are clearly reduced (typically~ 0.3%), as compared to the inter-chain V–V separation. This intra-chain compression is reflected in the contraction of the c-axis lattice parameter, and is likely produced by the introduction of the smaller Y^{3+} ions. As a result, the conduction along the

Table 1
Vanadium–Vanadium distances in the CVO and Y-doped CYVO samples. V–V NN (nearest neighbor) indicates the V–V distance along the legs of the chains (between V ions linked through the d_{xy} orbitals, see Fig. 1). The distances between V ions in partner legs of a given chain (linked through the d_{xz} or d_{yz} orbitals, according to Fig. 1) is indicated by the V–V NNN (next-nearest neighbor) distance. Subindices 1 and 2 identify the two slightly different zig-zag chains present in the structural primitive cell [5]. V_1–V_2 is the distance between V ions in different chains (along both crystallographic directions, a and b).

Sample	CaV_2O_4	$Ca_{0.9}Y_{0.1}V_2O_4$
V_1–V_1 NN (Å)	3.014	3.008
V_1–V_1 NNN (Å)	3.094	3.081
V_2–V_2 NN (Å)	3.014	3.008
V_2–V_2 NNN (Å)	3.081	3.073
V_1–V_2 along a (Å)	3.648	3.644
V_1–V_2 along b (Å)	3.575	3.588

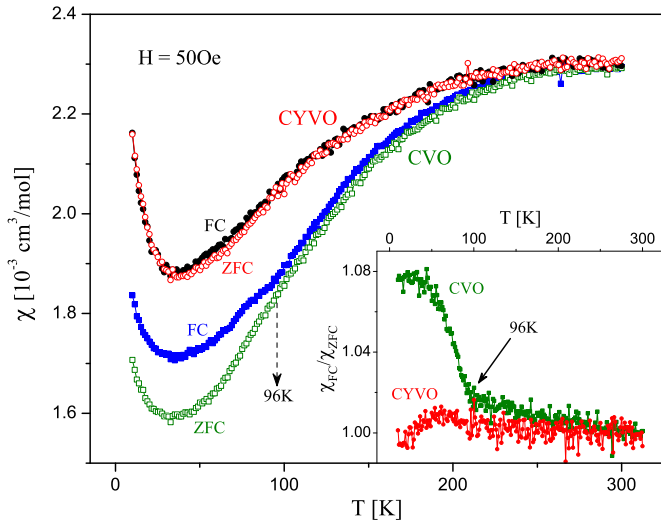**Fig. 4.** Susceptibility vs. temperature for CaV_2O_4 and $Ca_{0.9}Y_{0.1}V_2O_4$ measured with a field of 50 Oe, after field cooling (FC) and zero-field cooling (ZFC) processes. Inset: The ratio χ_{FC}/χ_{ZFC} vs. T for both samples.

chains is naturally enhanced in CYVO, increasing the anisotropy of the system and likely producing a dimensional crossover.

The structural changes provide a natural explanation for the dimensional difference between the samples through the modification of the intra-chain connectivity. Nevertheless, the presence of strong disorder would affect also the perpendicular localization length, and some dependence with sample quality and preparation method is also expected [21]. Therefore, a deeper understanding of the transport mechanism in CaV_2O_4 requires further investigation.

3.2. Magnetic properties

Next we will show that V vacancies also have important consequences on the magnetism of CaV_2O_4. Fig. 4 shows the susceptibility (χ) as a function of temperature for the two samples, measured in a Quantum Design Squid magnetometer. These data were obtained by applying a small magnetic field $H = 50$ Oe, on warming between 10 K and 300 K after field-cooling (FC) and zero-field-cooling (ZFC) processes. At room T both samples reach a susceptibility of 2.3×10^{-3} cm^3/mol, similar to previous results in CVO. Around this temperature, the broad maximum has been attributed to frustrated magnetic interactions. In principle, the competing interactions J_ℓ and J_z could introduce frustration in this quasi-1D spin system. However, recent results suggest that $J_\ell \gg J_z$ due to the smaller electronic population of the d_{xz} and d_{yz} orbitals [5,6]. Thus, from the magnetic point of view in the room temperature orthorhombic structure the legs would behave as two independent $S=1$ (Haldane) chains with negligible frustration. In this case, the maximum susceptibility occurs at a temperature comparable to the AFM interaction J_ℓ. Due to the short correlation lengths, the Haldane state has been shown to be quite robust against the presence of nonmagnetic impurities [22]. This is indeed our observation for T above ~220 K, where the clean CVO and disordered CYVO samples coincide (see Fig. 4). Moreover, the almost completely reversible susceptibility ($\chi_{FC} \approx \chi_{ZFC}$) independent of the magnetic history of the samples also suggests (at most) just weakly frustrated magnetic interactions.

Unlike the high temperature response, the susceptibility at low temperatures is very different for both samples. While CYVO remains almost totally reversible, below $T \sim 96$ K the undoped CaV_2O_4 shows a large splitting between the FC and ZFC data (see Fig. 4). This splitting is accompanied by a clear kink in the field-

cooling $\chi(T)$ data at $T \sim 96$ K (similar features are observed at the order temperature in NaV_2O_4, Ref. [10]). According to Pieper et al. [6], for T below~110–140 K a monoclinic distortion removes the degeneracy between the d_{xz} and d_{yz} orbitals of V. As a result, one of these orbitals is emptied while the other one is fully occupied, leading to an AFM spin-ladder ground state [4–6], as depicted in Fig. 1. Therefore, the splitting between the FC and ZFC data of CVO at 96 K indicates the appearance of magnetic domain walls and anisotropy effects, i.e. it signals the onset of long-range ordered AFM domains. On the contrary, the CYVO sample containing V vacancies shows a very minor irreversibility, implying that a concentration of vacancies of ~0.65% is able to widely suppress the long-range magnetic order. This behavior is similar to the collapse of the spin-Peierls state in impurity-doped $CuGeO_3$ [22,23], and reflects a more general physics where spin models for low dimensional systems such as chains and ladders show a rapid suppression of the spin gap due to the addition of small amounts of nonmagnetic impurities [24]. Actually, this behavior is unique to low dimensional systems where long-range magnetic order (such as an AFM spin ladder) is extremely sensitive to disorder. Probably, undetectable amounts of defects are also responsible for the contradictory results about the magnetic ground state of CaV_2O_4 [3–7,21,25].

When a nonmagnetic impurity is added into an AFM spin ladder, one of the rungs is damaged leaving three "loose" spins without one of the AFM bonds (two neighbors in the same leg above and below the impurity and another one in the same rung). The consequence of this is a larger magnetic moment as compared to the clean material, as we indeed observe in Fig. 4 for CYVO. However, the effects of the vacancies and broken bonds on the surrounding spins are not clear. In order to explore these effects we measured isothermal magnetization (M) vs. H data of our samples, after FC and ZFC processes. These data reflect mostly linear $M(H)$ curves, coherent with the predominant AFM phase. However, when the CYVO sample is cooled with an applied field the $M(H)$ data show important differences with respect to the ZFC magnetization. In the inset of Fig. 5 we show the data at $T = 10K$, after cooling the sample from 325 K in zero field and with an applied field of 50 kOe. We present a blow up of $M(H)$ for $|H| \leq 4$ kOe, where the FC curve appears clearly shifted toward the negative field axis (or positive magnetization axis as well). This is the well known exchange bias (EB) effect, which originates in the
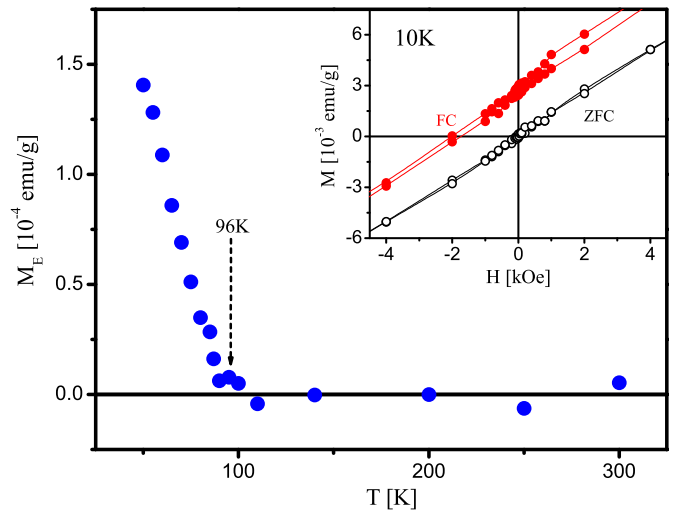

Fig. 5. Inset: $M(H)$ loops at 10 K for CYVO, after cooling the sample in zero field (ZFC) and with an applied field of 50 kOe (FC). The exchange bias effect is clearly seen in the FC data. Main panel: T dependence of the vertical shift of the remanent magnetization (M_E) obtained from $M(H)$ after cooling the sample with a field of 30 kOe.

interface exchange interaction between ferromagnetic and anti-ferromagnetic domains [26]. Therefore, the observation of EB in CYVO provides two important pieces of information: first that some AFM domains still survive in this sample, and second the sample must also contain regions with FM-like spin correlations in close contact with the AFM domains, as observed in other compounds [26,27].

We must mention that exchange bias is totally absent in CVO, thus V vacancies are at the root of the origin of the EB phenomena in CYVO [28]. Therefore, we postulate that each V vacancy induces a local net magnetization in its vicinity. Although not exactly the same case as our study, in spin-1/2 systems it has been calculated that spinless vacancies can affect the surrounding spins in several ways, such as enhancing the local susceptibility of the AFM spins and leaving uncompensated moments [24]. In fact, these end-chain spins with broken AFM bonds and their coupling across the vacancy site [29], as well as small changes in the local structural distortions [30], can promote local FM correlations. Within this picture, EB occurs due to a close interaction between AFM V chains and vacancy-induced magnetized regions. Then, EB should decrease with increasing T and eventually vanish at the Nèel temperature of the AFM phase. To study the temperature dependence of EB we measured several M–H loops at different temperatures. In this case we used a Vibrating Sample Magnetometer mounted on a cryogen-free system from Quantum Design, equipped with a 30 kOe magnet. We cooled the CYVO sample from 325 K down to 50 K with an applied field of 30 kOe. Then the temperature was raised to the value where $M(H)$ data were recorded. Quantification of EB was done through the vertical displacement of the remanent magnetization, M_E [27,31]. The M_E vs. T data shown in the main panel of Fig. 5 clearly demonstrate that, as expected, the EB effect decreases with increasing T and finally vanishes at temperatures close to 96 K. This coincides with the temperature below which long-range AFM order is established in the undoped CaV_2O_4, meaning that AFM order is not completely suppressed in CYVO. Although the average distance between vacancies in this sample is only 23 nm, the AFM domains responsible for the EB effect likely correspond to longer segments of chains that have some statistical probability to occur, and show AFM ordering below $\sim$ 96 K. Most of the sample, however, has short segments of V chains where long-range AFM order appears to be suppressed.

4. Conclusions

In conclusion, the $Ca_{0.9}Y_{0.1}V_2O_4$ compound shows the formation of V vacancies that chop the V *zig-zag* chains into small sections of length $\ell \approx 23$ nm. In this defective material, the observed VRH transport mechanism indicates that electron–electron interactions dominate the charge excitations, thus anisotropic long-range Coulomb interactions must be considered when studying the insulating properties of CaV_2O_4. Also, these vacancies change the V–V exchange interactions in their vicinity. While the high-temperature Haldane state remains robust, at low T the vacancies break the long-range order that occurs in the quasi-1D AFM CaV_2O_4. This is typical of low dimensional systems, where long-range magnetic order is extremely sensitive to disorder.

References

[1] I. Affleck, J. Phys: Condens. Matter 1 (1989) 3047; E. Dagotto, Rep. Prog. Phys. 62 (1999) 1525.
[2] B.F. Decker, J.S. Kasper, Acta Cryst. 10 (1957) 332; P.M. Hill, et al., Acta Cryst. 9 (1956) 981.
[3] H. Kikuchi, et al., Can. J. Phys. 79 (2001) 1551; H. Fukushima, et al., Prog. Theor. Phys. Suppl. 145 (2002) 72.
[4] X. Zong, et al., Phys. Rev. B 77 (2008) 014412.
[5] A. Niazi, et al., Phys. Rev. B 79 (2009) 104432.
[6] O. Pieper, et al., Phys. Rev. B 79 (2009) 180409.
[7] J.M. Hastings, et al., J. Phys. Chem. Solids 28 (1967) 1089.
[8] T. Hikihara, et al., Phys. Rev. B 63 (2001) 174430; M. Kaburagi, et al., J. Phys. Soc. Jpn. 68 (1999) 3185; T. Hikihara, Can. J. Phys. 79 (2001) 1593.
[9] A. Kolezhuk, et al., Phys. Rev. Lett. 77 (1996) 5142; S. Todo, et al., Phys. Rev. B 64 (2001) 224412.
[10] H. Sakurai, Phys. Rev. B 78 (2008) 094410.
[11] K. Yamaura, et al., Phys. Rev. Lett. 99 (2007) 196601.
[12] T. Qian, et al., J. Phys. Soc. Jpn. 78 (2009) 024709.
[13] M. Kasuya, et al., Phys. Rev. B 47 (1993) 6197.
[14] F. Cintolesi, et al., J. Appl. Phys. 79 (1996) 6624.
[15] N.F. Mott, E.A. Davis, Electronic processes, in: Non-Crystalline Materials, 2nd ed., 1979, Clarendon Press, Oxford.
[16] B.I. Shklovskii, A.L. Efros, Electronic Properties of Doped Semiconductors, Springer, New York, 1984; A.L. Efros, B.I. Shklovskii, J. Phys. C 8 (1975) L49.
[17] M.M. Fogler, et al., Phys. Rev. B 69 (2004) 035413.
[18] The term "soft" Coulomb gap refers to the fact that the density of states $g(\varepsilon)$ actually vanishes only at the Fermi level, and slowly increases with a power-law dependence for energies close to ε_F.
[19] S. Kirkpatrick, Rev. Mod. Phys. 45 (1973) 574; I. Webman, et al., Phys. Rev. B 14 (1976) 4737.
[20] D.C. Johnston, et al., in: A. Fujimori, Y. Tokura (Eds.), Spectroscopy of Mott Insulators and Correlated Metals, Springer Series in Solid-State Sciences, vol. 119, Springer-Verlag, Berlin Heidelberg, 1995, p. 241, and references therein.
[21] H. Sakurai, et al., J. Phys.: Conf. Ser. 273 (2011) 012119.
[22] Y. Ajiro, et al., Phys. Rev. B 51 (1995) 9399.
[23] M. Hase, et al., Phys. Rev. Lett. 71 (1993) 4059.
[24] M. Laukamp, et al., Phys. Rev. B 57 (1998) 10755.
[25] M. Azuma, et al., Phys. Rev. B 55 (1997) R8658.
[26] For reviews see for example, S. Giri, et al., J. Phys.: Condens. Matter 23 (2011) 073201; J. Nogués, I.K. Schuller, J. Magn. Magn. Mater. 192 (1999) 203.
[27] D. Niebieskikwiat, M.B. Salamon, Phys. Rev. B 72 (2005) 174422.
[28] We note that, with the high purity raw materials used for the sample preparation (99.999%), FM impurities in these chemicals can be ruled out as the origin of the FM component. A thorough calculation indicates that the remanent magnetization in the FC curve in the inset of Fig. 5 is at least two orders of magnitude larger than all possible FM iron impurities could contribute.
[29] A. Zorko, et al., Phys. Rev. B 73 (2006) 104436.
[30] G.-W. Chern, N. Perkins, Phys. Rev. B 80 (2009) 220405.
[31] In samples with small FM regions immersed within a dominant AFM matrix, quantification of the EB field (the displacement of the M–H loop to the left of the origin) is very unreliable due to its large sensitivity to the AFM contribution that must be subtracted from $M(H)$. However, an alternative description of EB can be done through the vertical shift of the remanence, which does not require any manipulation of the data (see D. Niebieskikwiat, M.B. Salamon, Phys. Rev. B 72 (2005) 174422).